ACS Catalysis

Research Article

Cite This: ACS Catal. 2019, 9, 1464−1471

pubs.acs.org/acscatalysis

An $n\rightarrow\pi^*$ Interaction in the Bound Substrate of Aspartic Proteases Replicates the Oxyanion Hole

Ian W. Windsor, Brian Gold, and Ronald T. Raines*

Department of Chemistry, Massachusetts Institute of Technology, Cambridge, Massachusetts 02139, United States

Supporting Information

ABSTRACT: Aspartic proteases regulate many biological processes and are prominent targets for therapeutic intervention. Structural studies have captured intermediates along the reaction pathway, including the Michaelis complex and tetrahedral intermediate. Using a Ramachandran analysis of these structures, we discovered that residues occupying the P1 and P1′ positions (which flank the scissile peptide bond) adopt the dihedral angle of an inverse γ-turn and polyproline type-II helix, respectively. Computational analyses reveal that the polyproline type-II helix engenders an $n\rightarrow\pi^*$ interaction in which the oxygen of the scissile peptide bond is the donor. This interaction stabilizes the negative charge that develops in the tetrahedral intermediate, much like the oxyanion hole of serine proteases. The inverse γ-turn serves to twist the scissile peptide bond, vacating the carbonyl π^* orbital and facilitating its hydration. These previously unappreciated interactions entail a form of substrate-assisted catalysis and offer opportunities for drug design.

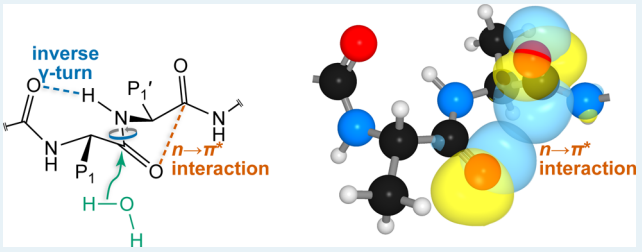

KEYWORDS: *aspartic protease, HIV-1 protease, inverse γ-turn, n→π* interaction, oxyanion hole, pepsin, renin, substrate-assisted catalysis*

INTRODUCTION

Aspartic proteases (EC 3.4.23) have played a central role in the history of protein science. The human digestive enzyme pepsin was the subject of seminal studies in mechanistic enzymology and protein crystallography.[1] Fueled by aspartic proteases being therapeutic targets, endothiapepsin and HIV-1 protease emerged as model systems and together account for over 1,000 entries in the Protein Data Bank. In accord with a common reaction mechanism, aspartic proteases share susceptibility to inhibition by the peptidic natural product pepstatin. Its hydroxyethylene pharmacophore, which mimics an intermediate in the enzyme-catalyzed reaction, forged the route to clinical inhibitors of aspartic proteases.[2]

Aspartic proteases employ a pair of aspartic acid residues to activate a water molecule for nucleophilic attack on a peptide bond. This catalytic dyad arises from a pair of "DTG" motifs at the interface between two globular domains (Figure 1A).[3] Eukaryotic aspartic proteases are monomeric and consist of two unique domains,[4] whereas retroviral homologues are homodimeric (Figures 1B and 1C).[5] In addition to the DTG motifs, aspartic proteases share other structural elements, including a β-barrel domain and flap that close upon polypeptide substrates. The enzymes vary, however, in their substrate promiscuity and biological niche. For example, renin cleaves angiotensinogen with exquisite specificity to elicit vasoconstriction,[6] whereas HIV-1 protease recognizes a variety of substrates to enable maturation of new virions.[7]

The catalytic mechanism of retroviral proteases has been informed by the use of substrate mimetics[8] and, especially, inactive variants. In seminal work, Wlodawer and co-workers employed site-directed mutagenesis to inactivate FIV protease and then determined the structure of the inactive variant bound to an actual substrate.[9] Schiffer and co-workers extended this strategy to HIV-1 protease while developing their shape-complementary model of side chain recognition.[10]

Typically, the main chain conformation of the substrates of aspartic proteases is thought to resemble that of a β-strand.[11] We have examined the structures of inactivated protease·substrate complexes, focusing on the main chain. We have discovered that the substrates do not resemble a β-strand near the scissile peptide bond. Instead, the substrate adopts a conformation in which the oxygen of the scissile peptide bond donates electron density via an $n\rightarrow\pi^*$ interaction to the next carbonyl group in the main chain. The discovery of this interaction, as well as the formation of an inverse γ-turn within the substrate, suggests that aspartic proteases rely on substrate-assisted catalysis[14] to effect the cleavage of peptide bonds.

RESULTS AND DISCUSSION

We began our investigation of the role of main chain conformation in the mechanism of aspartic proteases by gathering structures of substrates bound to inactivated enzymes.[15] Since 1997, 35 structures of inactivated retroviral proteases with flaps closed on peptidic substrates have been

Received: October 13, 2018
Revised: November 19, 2018
Published: November 29, 2018

DOI: 10.1021/acscatal.8b04142
ACS Catal. 2019, 9, 1464−1471

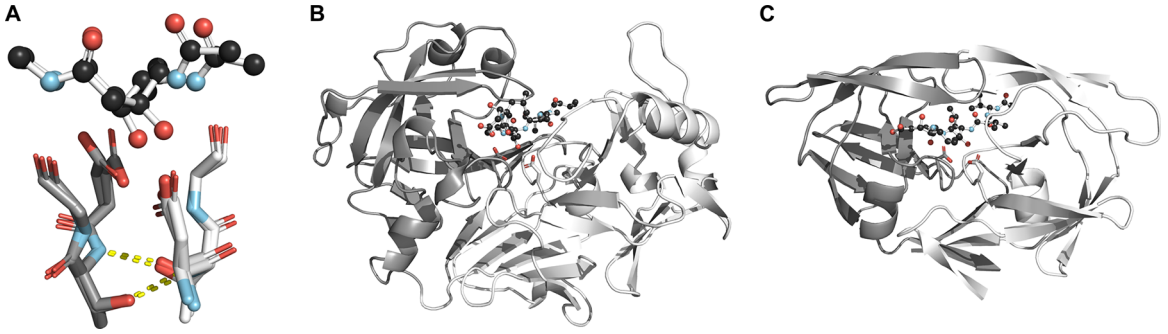

Figure 1. Structural features of aspartic proteases. (A) Aspartic proteases share the "DTG" motif with an interdomain hydrogen bond. Here, the residues from a eukaryotic pepsin (PDB entry 1pso[12]) and HIV-1 protease (PDB entry 5hvp[13]) are aligned with an RMSD of 0.272 Å. (B) The eukaryotic pepsin consists of two unique domains and has only one flap. (C) HIV-1 protease consists of identical monomers that associate with 2-fold symmetry.

deposited in the PDB (Table S1).[9,10,16] Next, we measured the ϕ and ψ angles of residues in the P1 and P1′ position to generate a Ramachandran plot (Figure 2). The peptide bond

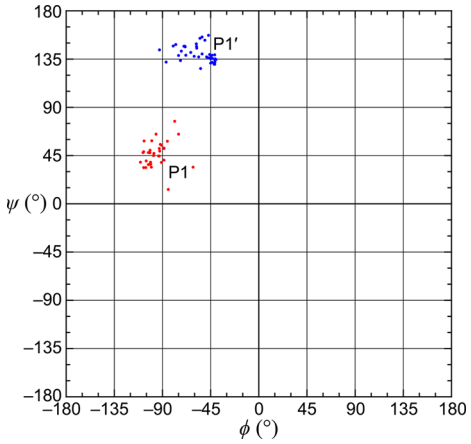

Figure 2. Ramachandran plot of P1 and P1′ residues in substrates bound to the active site of inactivated aspartic proteases.

between these two residues is the one cleaved by the enzymes. We found distinct clusters of P1 and P1′ residues, with mean values of $\phi = -95.5° \pm 10.1°$ and $\psi = 44.9° \pm 10.4°$ for P1 residues, and $\phi = -56.3° \pm 14.5°$ and $\psi = 140.0° \pm 7.5°$ for P1′ residues.

Conformation of the P1 Residue. The P1 residue of bound substrates adopts conformations in the broad region of the Ramachandran plot associated with β-strands. An analysis by Rose and co-workers identified a subset of this region with ϕ angles between −100° to −70° and ψ angles between 50° to 100° populated by members of a coil-library that contains an inverse γ-turn, called the "γ-basin" (Figure 3A).[17] Its signature inverse γ-turn motif was described nearly a half-century ago[18] and is characterized by a hydrogen bond between the $i - 1$ main chain oxygen and $i + 1$ main chain nitrogen, forming a 7-membered ring.[19] The donor−acceptor angle deviates from linearity, making the hydrogen-bond energies of inverse γ-turns weaker than those of other secondary structural elements, such as β-turns and β-sheets. The inverse γ-turn centered on the P1 residue results from the P2 ($i - 1$) residue accepting a hydrogen bond from the P1′ ($i + 1$) residue (Figure 3B). β-Branched amino acids are excluded from inverse γ-turns, as their side chain would clash with the main chain nitrogen of residue i.[17] Notably, the incorporation of β-branched residues at the P1 position yields inefficient substrates for HIV-1 protease, consistent with the importance of an inverse γ-turn conformation for catalysis.[20]

An inverse γ-turn is incompatible with the 1 of endogenous HIV protease substrates that contain a P1′ proline residue, which lacks the requisite main chain N−H.[21] Segregating the P1 Ramachandran plot based on sequence revealed to us that substrates with a P1′ proline residue have expanded ϕ angles that move the conformation of the P1 residue out of the γ-basin (Figure 3A). These structures have intramolecular hydrogen bonds between the side chains of the P2 and P4 residues (Figure 3C). Their proline-containing substrates all have P2 and P4 residues with polar groups, which could serve to increase the ϕ angle and move the P2 carbonyl group away from the P1′ pyrrolidine ring. An asparagine residue is found most commonly at the P2 position of substrates with a P1′ proline residue but is also found at the P2 position of those substrates known as "p1/p6". In p1/p6 substrates, the side chain oxygen of the asparagine residue, rather than its main chain oxygen, accepts a hydrogen bond from the $i + 1$ main chain nitrogen (Figure 3D).[16g] In addition to an increased ϕ angle, the P1 residue of p1/p6 substrates exhibits a reduced ψ angle, which serves to rotate the main chain N−H toward the side chain of the asparagine residue in the P2 position (Figure 3A).

The inverse γ-turn in the main chain of P1 residues has not gone unnoticed. Medicinal chemists, guided by knowledge that proline is often found in inverse γ-turns, discovered that replacing the main chain of substrates at the P2 to P1′ positions with a seven-membered ring can generate potent inhibitors of HIV protease.[22] Although this strategy was intended to mimic the inverse γ-turn, structural analyses revealed that the ring shifted by a "half" residue relative to that in substrates.[23]

Conformation of the P1′ Residue. The main chain of the P1′ residue occupies a region of the Ramachandran plot associated with the polyproline type-II (PPII) helix (Figure 4A) and exhibits structural features conducive for preorganization (Figure 4B, Table S1). Comparing the main chain dihedral angles of P1′ residues (Figure 4C) with the structure of a PPII helix solved by Wennemers and co-workers using direct methods reveals a striking similarity (Figure 4D).[24] The lack of hydrogen bond-donating groups in the main chain of polyproline entices donation of oxygen electron density to an alternative acceptor—the π^* orbital of the $i + 1$ carbonyl group.[25] (For reviews of the $n \rightarrow \pi^*$ interaction, see ref 26.) In

DOI: 10.1021/acscatal.8b04142
ACS Catal. 2019, 9, 1464−1471

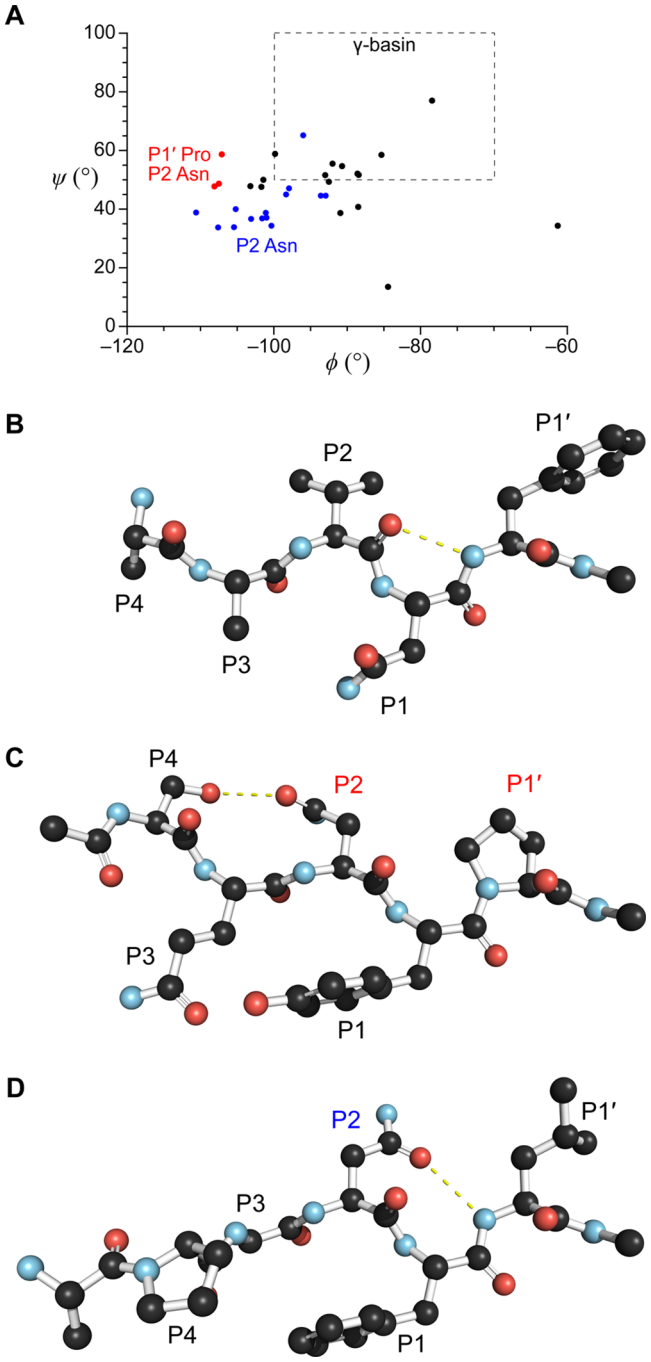

Figure 3. Main chain conformation of the P1 residue. (A) Ramachandran plot of P1 residues in substrates bound to the active site of inactivated aspartic proteases. Data points are colored by the presence of a proline residue at the P1′ position and an asparagine residue at the P2 position (red), an asparagine residue at the P2 position (blue), or neither (black). All data points are shown relative to the γ-basin. (B) The P2, P1, and P1′ residues engage in an inverse γ-turn (NC/p1 substrate; PDB entry 1tsq).[16b] (C) A proline residue at the P1′ position precludes the formation of an inverse γ-turn but is found with polar residues at the P2 and P4 positions that form hydrogen bonds (MA/CA substrate; PDB entry 1mt7).[16a] (D) The side chain of an asparagine residue at the P2 position forms a hydrogen bond with the nitrogen of the scissile peptide bond (p1/p6 substrate; PDB entry 4obf).[16g]

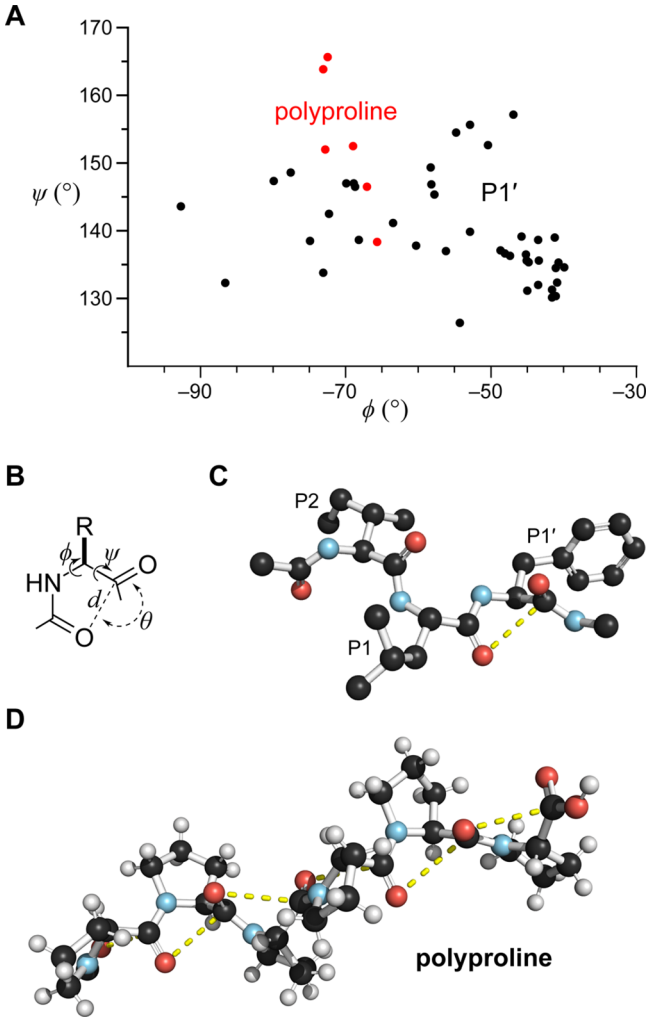

Figure 4. Main chain conformation of the P1′ residue. (A) Ramachandran plot of P1′ residue substrates bound to the active site of inactivated aspartic proteases (black) and the residues in a PPII helix (red).[24] (B) Parameters used to assess $n\rightarrow\pi^*$ interactions between adjacent main chain carbonyl groups in a protein (Tables S1 and S2). (C) Structure of a P1 residue bound to an inactivated HIV-1 protease and showing its $n\rightarrow\pi^*$ interaction (PDB entry 1kjh; d = 3.0 Å, θ = 95.4°).[10b] (D) Structure of a polyproline fragment showing its $n\rightarrow\pi^*$ interactions (CSD entry SOWJUL; d = 3.1 Å ± 0.1 Å, θ = 97.4° ± 7.2°).[24]

α-helices, donor carbonyl groups employ $n\rightarrow\pi^*$ interactions with the *si* face of the adjacent carbonyl group, whereas in PPII helices the interaction is with the *re* face. Previous systematic, energetic analysis by our group estimated that a residue occupying the dihedral angle near the average for residues in the P1′ position (ϕ = −55° and ψ = 140.0°) has an $n\rightarrow\pi^*$ interaction with an energy of 1.0 kcal/mol.[27]

The PPII-helical conformation is not limited to proline-rich sequences. Unfolded protein sequences likewise occupy this conformation.[28] Protease substrates must be sufficiently disordered to avoid adopting a secondary structural element such as an α-helix or β-sheet, which would preclude binding, but must adopt a conformation complementary to the enzymic active site.[29] An analysis by Brown and Zondlo identified proline, leucine, and alanine as the residues with the greatest propensity to form PPII helices when flanked by pairs of proline residues.[30] These three amino acids constitute half of the P1′ residues in endogenous substrates. Their analysis also identified β-branched and small polar residues as being

DOI: 10.1021/acscatal.8b04142
ACS Catal. 2019, 9, 1464−1471

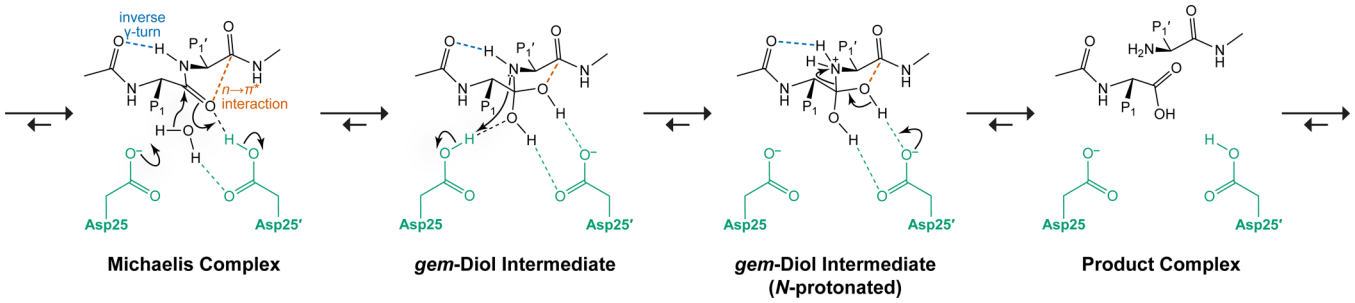

Figure 5. Putative mechanism of catalysis by HIV-1 protease. The hydrolysis reaction proceeds through at least three discrete steps. Upon binding the peptidic substrate and lytic water, Asp25 of one monomer deprotonates the water while Asp25′ of the other monomer transfers a proton to the oxygen of the scissile peptide bond. This oxygen also forms an $n\rightarrow\pi^*$ interaction (red dashed line) with the main chain carbonyl group of the next residue in the substrate. The $n\rightarrow\pi^*$ interaction is even stronger in the tetrahedral intermediate. The inverse γ-turn (blue dashed line) disturbs the planarity of the scissile peptide bond and orients the nitrogen lone pair for protonation by Asp25.

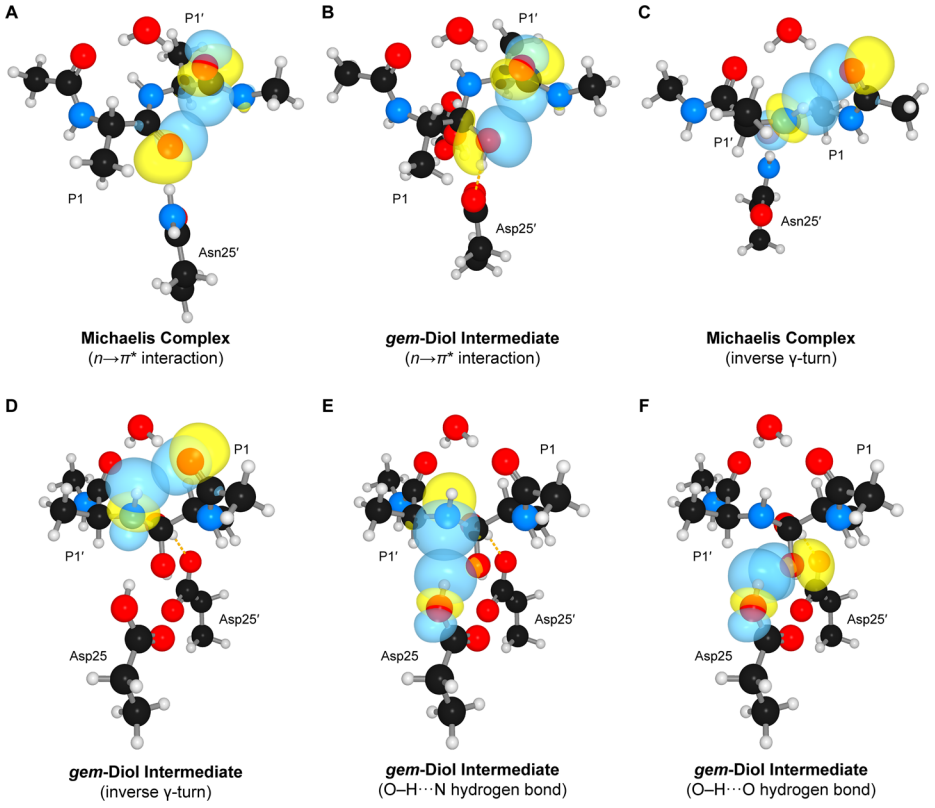

Figure 6. Orbital interactions of the scissile peptide bond during catalysis by HIV-1 protease. An $n\rightarrow\pi^*$ interaction occurs within the substrate (A) and tetrahedral intermediate (B). An inverse γ-turn likewise forms within the substrate (C) and tetrahedral intermediate (D). The hydrogen bond of the inverse γ-turn enforces a hydrogen bond between the lone pair of the nitrogen of the scissile peptide bond and an active-site aspartic acid residue (E), despite a competing hydrogen bond of the aspartic acid residue with the *gem*-diol (F).

disfavored in a PPII helix, and those residues lead to inefficient substrates of HIV-1 protease when in the P1′ position.[31]

Mechanistic Insights. Informed by our bioinformatics analysis, we sought insight on the catalytic mechanism of aspartic proteases. The catalytic mechanism of amide hydrolysis proceeds first via nucleophilic attack of water at the P1 carbonyl group to generate a tetrahedral intermediate that is a geminal diol (Figure 5). Proteolytic cleavage is completed upon protonation of the P1′ nitrogen and subsequent C−N bond scission. To investigate this mechanism, we performed quantum chemical calculations on coordinates extracted from high-resolution cocrystal structures of a substrate and a *gem*-diol intermediate bound to HIV-1 protease. To represent the Michaelis complex, we chose a recent cocrystal structure of a highly efficient substrate bound to an inactivated protease (PDB entry 6bra[32]), which has the highest resolution of any such structure. To represent the *gem*-diol intermediate, we chose a structure by Weber and coworkers that employed threonine as the P1′ residue (PDB entry 3b80[31]).

When extracting coordinates, we sought to preserve noncovalent interactions between the P2/P1 and the P1′/P2′ carbonyl groups near the scissile peptide bond. To do so, we extracted the coordinates of the P1 and P1′ residues to the β-carbon of their side chains, the distal amides and C^{α} atoms from the P2 and P2′ residues along with a conserved water molecule, the main chain amides of the protease flap that form hydrogen bonds with the conserved water molecule, and the

DOI: 10.1021/acscatal.8b04142
ACS Catal. 2019, 9, 1464−1471

aspartic acid or asparagine side chains of protease residues 25 and 25′. Next, we optimized the positions of hydrogen atoms with density functional theory (DFT) calculations. Hydrogen atoms were added to the structure to create a neutral structure of the Michaelis complex and a monoanionic structure of the tetrahedral intermediate. There was no ambiguity in assigning hydrogen atoms in the substrate structures. The protonation of the *gem*-diol intermediate was modeled to match neutron diffraction structures in which both hydroxy groups form hydrogen bonds with an aspartate residue,[33] as is proposed for the tetrahedral intermediate. Finally, we performed Natural Bonding Orbital (NBO) analysis of the ensuing models to estimate the strength of noncovalent interactions.[34]

In the Michaelis complex, the inverse γ-turn−PPII-like motif activates the π^* orbital of the P1 carbonyl group for nucleophilic attack by water. The two flanking carbonyl groups (i.e., those of the P2 and P1′ residues) form hydrogen bonds, either with a conserved water molecule in retroviral proteases or with the flap of monomeric proteases. The ensuing constraint increases the electrophilicity of the P1 carbonyl group by both enhancing the $n\rightarrow\pi^*$ interaction with the P1′ carbonyl group and preventing $n\rightarrow\pi^*$ donation from the P2 carbonyl group, which would otherwise raise the energy of the π^* orbital of the P1 carbonyl group and diminish its electrophilicity.[35]

As the reaction proceeds to the tetrahedral intermediate, the $n\rightarrow\pi^*$ interaction grows stronger, increasing from 0.66 to 2.01 kcal/mol. This latter energy, which is remarkably high, serves to delocalize developing negative charge (Figure 6A and 6B). Thus, the $n\rightarrow\pi^*$ interaction between the P1 and P1′ carbonyl groups effectively acts like the renowned oxyanion hole of serine proteases, which delocalizes developing negative charge through the formation of a pair of hydrogen bonds with enzymic N−H groups.[36] As has been postulated for hydrogen-bonding with the oxyanion hole,[36a,37] the $n\rightarrow\pi^*$ interaction is stronger in the tetrahedral intermediate than in the Michaelis complex. This differential binding of the Michaelis complex and tetrahedral intermediate is likely to enhance catalysis.[38]

Like the $n\rightarrow\pi^*$ interaction, the inverse γ-turn is important in the enzymatic reaction mechanism. In the first step, amidic resonance must be overcome. At first glance, a hydrogen bond to the main chain nitrogen of the P1′ residue might be thought to increase amidic resonance and thereby decrease the electrophilicity of the scissile peptide bond. Upon forming the inverse γ-turn, however, the scissile peptide bond is twisted out of plane, decreasing amidic resonance and increasing electrophilicity.[39] In the Michaelis complex, the amide nitrogen is pyramidalized slightly and the lone pair hybridizes to a small degree (∼3% *s*-character, versus <1% *s*-character in adjacent amides) because of the inverse γ-turn hydrogen bond, which has an energy of a 0.66 kcal/mol (Figure 6C). This interaction is absent in substrates that have proline in the P1′ position, and these substrates are cleaved only slowly by the protease.[40] Similarly, the asparagine side chain in the P2 position of the p1/p6 substrate competes for the γ-turn, resulting in efficient cleavage.[41]

In the tetrahedral intermediate, the energy of the inverse γ-turn hydrogen bond is maintained at 0.67 kcal/mol (Figure 6D). Although the scissile peptide bond is now hydrated, its nitrogen lone pair still contains only ∼7% *s*-character, which is much less than the 25% *s*-character of an sp^3-hybridized orbital. We find that the low hybridization is due to the presence of the neighboring *gem*-diol, in which a higher energy *p*-rich lone pair of the nitrogen is a better donor of electron density to the two σ^*_{C-O} orbitals. Nonetheless, the inverse γ-turn also aligns the nitrogen lone pair toward the protonated oxygen of Asp25, resulting in a hydrogen bond with an energy of 0.79 kcal/mol (Figure 6E). This aspartic acid residue also maintains a hydrogen bond of energy 5.36 kcal/mol with the *gem*-diol (Figure 6F). As the proton transfer to the N−H proceeds, the energies of the two $n_N\rightarrow\sigma^*_{C-O}$ interactions likely decrease and the energy of the $n_O\rightarrow\sigma^*_{C-N}$ interaction likely increases, promoting C−N bond scission to form the products.

Computational chemists have devoted much attention to the catalytic mechanism of aspartic acid proteases, especially that of HIV-1 protease.[42] These studies have tended to employ a hybrid quantum mechanical/molecular mechanical (QM/MM) approach in which the higher level of theory is used to describe molecular fragments that are smaller than those analyzed herein.[43] Our findings suggest that previous analyses have missed critical details: the $n\rightarrow\pi^*$ interaction and inverse γ-turn. New computational strategies are needed to select fragments that capture all of the interactions that make significant contributions to catalysis by aspartic acid proteases and other enzymes.[44]

CONCLUSIONS

Ramachandran analysis of the residues in substrates bound to aspartic proteases has revealed previously unappreciated noncovalent interactions. When bound, the substrate adopts a conformation with an $n\rightarrow\pi^*$ interaction and an inverse γ-turn, both of which activate the scissile peptide bond for nucleophilic attack by a water molecule. To our knowledge, the use of these interactions in substrate-assisted catalysis had not been described previously. Notably, these findings extend the reach of $n\rightarrow\pi^*$ interactions between adjacent main chain carbonyl groups to enzymatic catalysis.[45]

EXPERIMENTAL SECTION

Structural Analyses. The atomic coordinates of X-ray crystal structures that were deposited in the Protein Data Bank as of August 9, 2018 and that contain inactivated retroviral aspartic proteases were downloaded. The structure SOWJUL[24] was downloaded from the Cambridge Structural Database. Angles and distances in these structures were measured to the nearest 0.1 Å and 0.1°, respectively, with the program PyMOL from Schrödinger (New York, NY). Structures containing multiple protease dimers in the asymmetric unit or alternative conformations within a single protease molecule were measured individually and given equal weight in calculations of the mean. PDB codes and chain identifiers are listed in Table S1 along with the measured values. Structures were depicted with the program PyMOL.

DFT Optimization. Atoms important for determining the conformation of the scissile peptide bond in the Michaelis complex and *gem*-diol intermediate were extracted from PDB entries 6bra[32] and 3b80,[31] respectively. All termini were made into amides. Hydrogen atoms were added to extracted structures in idealized geometries with the program GaussView 6 from Gaussian (Wallingford, CT) and optimized at the M06-2X/6-311+G(d,p) level of theory along with the integral equation formalism variant of the polarizable continuum model (IEFPCM) for water-solvation[46] by using Gaussian 16, Revision A.03 software from Gaussian.[47] Optimized structure coordinates are listed in Tables S3 and S4.

DOI: 10.1021/acscatal.8b04142
ACS Catal. 2019, 9, 1464−1471

NBO Analysis. Optimized structures were subjected to natural bonding orbital analysis using the NBO 6.0 software from the Theoretical Chemistry Institute of the University of Wisconsin−Madison (Madison, WI).[48] Orbital interaction energies were calculated by second-order perturbation analysis. Orbitals were depicted with the program NBOView 1.1.[49]

■ ASSOCIATED CONTENT

Supporting Information

The Supporting Information is available free of charge on the ACS Publications website at DOI: 10.1021/acscatal.8b04142.

PDB entries and measured parameters, measured parameters from CSD entry SOWJUL, coordinates extracted from PDB entry 6bra and optimized hydrogen atoms, and coordinates extracted from PDB Entry 3b80 and optimized hydrogen atoms (PDF)

■ AUTHOR INFORMATION

Corresponding Author

*E-mail: rtraines@mit.edu. Tel: 617-253-1470.

ORCID

Brian Gold: 0000-0002-3534-1329

Ronald T. Raines: 0000-0001-7164-1719

Notes

The authors declare no competing financial interest.

■ ACKNOWLEDGMENTS

B.G. was supported by an Arnold O. Beckman Postdoctoral Fellowship. This work was supported by Grant R01 GM044783 (NIH). Calculations made use of the Molecular Graphics and Computational Facility at the University of California, Berkeley, which was supported by Grant S10 OD023532 (NIH).

■ REFERENCES

(1) (a) Knowles, J. R. On the Mechanism of Action of Pepsin. *Philos. Trans. R. Soc., B* **1970**, *B257*, 135−146. (b) Fruton, J. S. A. History of Pepsin and Related Enzymes. *Q. Rev. Biol.* **2002**, *77*, 127−147.

(2) (a) Boger, J.; Lohr, N. S.; Ulm, E. H.; Poe, M.; Blaine, E. H.; Fanelli, G. M.; Lin, T.-Y.; Payne, L. S.; Schorn, T. W.; LaMont, B. I.; Vassil, T. C.; Stabilito, I. I.; Veber, D. F.; Rich, D. H.; Bopari, A. S. Novel Renin Inhibitors Containing the Amino Acid Statine. *Nature* **1983**, *303*, 81−84. (b) Brik, A.; Wong, C. H. HIV-1 Protease: Mechanism and Drug Discovery. *Org. Biomol. Chem.* **2003**, *1*, 5−14.

(3) Dunn, B. M.; Goodenow, M. M.; Gustchina, A.; Wlodawer, A. Retroviral Proteases. *Genome Biol.* **2002**, *3*, reviews3006.1−3006.7.

(4) Dunn, B. M. Structure and Mechanism of the Pepsin-Like Family of Aspartic Peptidases. *Chem. Rev.* **2002**, *102*, 4431−4458.

(5) (a) Wlodawer, A.; Gustchina, A. Structural and Biochemical Studies of Retroviral Proteases. *Biochim. Biophys. Acta, Protein Struct. Mol. Enzymol.* **2000**, *1477*, 16−34. (b) Li, M.; Dimaio, F.; Zhou, D.; Gustchina, A.; Lubkowski, J.; Dauter, Z.; Baker, D.; Wlodawer, A. Crystal Structure of XMRV Protease Differs from the Structures of Other Retropepsins. *Nat. Struct. Mol. Biol.* **2011**, *18*, 227−229.

(6) (a) Green, D. W.; Aykent, S.; Gierse, J. K.; Zupec, M. E. Substrate Specificity of Recombinant Human Renal Renin: Effect of Histidine in the P2 subsite on pH Dependence. *Biochemistry* **1990**, *29*, 3126−3133. (b) Zhou, A.; Carrell, R. W.; Murphy, M. P.; Wei, Z.; Yan, Y.; Stanley, P. L. D.; Stein, P. E.; Broughton Pipkin, F.; Read, R. J. A Redox Switch in Angiotensinogen Modulates Angiotensin Release. *Nature* **2010**, *468*, 108−111.

(7) Tözsér, J. Comparative Studies on Retroviral Proteases: Substrate Specificity. *Viruses* **2010**, *2*, 147−165.

(8) Miller, M.; Schneider, J.; Sathyanarayana, B. K.; Toth, M. V.; Marshall, G. R.; Clawson, L.; Selk, L.; Kent, S. B. H.; Wlodawer, A. Structure of Complex of Synthetic HIV-1 Protease with a Substrate-Based Inhibitor at 2.3 Å Resolution. *Science* **1989**, *246*, 1149−1152.

(9) Laco, G. S.; Schalk-Hihi, C.; Lubkowski, J.; Morris, G.; Zdanov, A.; Olson, A.; Elder, J. H.; Wlodawer, A.; Gustchina, A. Crystal Structures of the Inactive D30N Mutant of Feline Immunodeficiency Virus Protease Complexed with a Substrate and an Inhibitor. *Biochemistry* **1997**, *36*, 10696−10708.

(10) (a) Prabu-Jeyabalan, M.; Nalivaika, E.; Schiffer, C. A. How Does a Symmetric Dimer Recognize an Asymmetric Substrate? A Substrate Complex of HIV-1 Protease. *J. Mol. Biol.* **2000**, *301*, 1207−1220. (b) Prabu-Jeyabalan, M.; Nalivaika, E.; Schiffer, C. A. Substrate Shape Determines Specificity of Recognition for HIV-1 Protease: Analysis of Crystal Structures of Six Substrate complexes. *Structure* **2002**, *10*, 369−381.

(11) Tyndall, J. D.; Nall, T.; Fairlie, D. P. Proteases Universally Recognize Beta Strands in Their Active Sites. *Chem. Rev.* **2005**, *105*, 973−999.

(12) Fujinaga, M.; Chernaia, M. M.; Tarasova, N. I.; Mosimann, S. C.; James, M. N. The Crystal Structure of Human Pepsin and Its Complex with Pepstatin. *Protein Sci.* **1995**, *4*, 960−972.

(13) Fitzgerald, P. M.; McKeever, B. M.; VanMiddlesworth, J. F.; Springer, J. P.; Helmbach, J. C.; Leu, C.-T.; Herger, W. K.; Dixon, R. A.; Darke, P. L. Crystallographic Analysis of a Complex Between Human Immunodeficiency Virus Type 1 Protease and Acetyl-Pepstatin at 2.0-Å resolution. *J. Biol. Chem.* **1990**, *25*, 14209−14219.

(14) Dall'Acqua, W.; Carter, P. Substrate-Assisted Catalysis: Molecular Basis and Biological Significance. *Protein Sci.* **2000**, *9*, 1−9.

(15) The legitimacy of this approach is supported by the structure of the inactive D25N protease·substrate complex being nearly identical to that of the complex formed by the wild-type protease and a substrate mimetic in which the scissile peptide bond is reduced to a secondary amine. For example, the inverse γ-turn is retained in the latter complex: Sayer, J. M.; Liu, F.; Ishima, R.; Weber, I. T.; Louis, J. M. Effect of the Active Site D25N Mutation on the Structure, Stability, and Ligand Binding of the Mature HIV-1 Protease. *J. Biol. Chem.* **2008**, *283*, 13459−13270.

(16) (a) Prabu-Jeyabalan, M.; Nalivaika, E. A.; King, N. M.; Schiffer, C. A. Viability of Drug-Resistant Human Immunodeficiency Virus Type 1 Protease Variant: Structural Insights for Better Antiviral Therapy. *J. Virol.* **2003**, *77*, 1306−1315. (b) Prabu-Jeyabalan, M.; Nalivaika, E. A.; King, N. M.; Schiffer, C. A. Structural Basis for Coevolution of a Human Immunodeficiency Virus Type 1 Nucleocapsid-p1 Cleavage Site with a V82A Drug-Resistant Mutation in Viral Protease. *J. Virol.* **2004**, *78*, 12446−12454. (c) Prabu-Jeyabaian, M.; Nalivaika, E. A.; Romano, K.; Schiffer, C. A. Mechanism of Substrate Recognition by Drug-Resistant Human Immunodeficiency Virus Type 1 Protease Variants Revealed by a Novel Structural Intermediate. *J. Virol.* **2006**, *80*, 3607−3616. (d) Altman, M. D.; Nalivaika, E. A.; Prabu-Jeyabalan, M.; Schiffer, C. A.; Tidor, B. Computational Design and Experimental Study of Tighter Binding Peptides to an Inactivated Mutant of HIV-1 Protease. *Proteins: Struct., Funct., Genet.* **2008**, *70*, 678−694. (e) Tyndall, J. D.; Pattenden, L. K.; Reid, R. C.; Hu, S. H.; Alewood, D.; Alewood, P. F.; Walsh, T.; Fairlie, D. P.; Martin, J. L. Crystal Structures of Highly Constrained Substrate and Hydrolysis Products Bound to HIV-1 Protease. Implications for the Catalytic Mechanism. *Biochemistry* **2008**, *47*, 3736−3744. (f) Bandaranayake, R. M.; Prabu-Jeyabalan, M.; Kakizawa, J.; Sugiura, W.; Schiffer, C. A. Structural Analysis of Human Immunodeficiency Virus Type 1 CRF01_AE Protease in Complex with the Substrate p1-p6. *J. Virol.* **2008**, *82*, 6762−6766. (g) Kolli, M.; Ozen, A.; Kurt-Yilmaz, N.; Schiffer, C. A. HIV-1 Protease−Substrate Coevolution in Nelfinavir Resistance. *J. Virol.* **2014**, *88*, 7145−7154. (h) Özen, A.; Lin, K.-H.; Kurt Yilmaz, N.; Schiffer, C. A. Structural Basis and Distal Effects of Gag Substrate Coevolution in Drug Resistance to HIV-1 Protease. *Proc. Natl. Acad. Sci. U. S. A.* **2014**, *111*, 15993−15998.

DOI: 10.1021/acscatal.8b04142
ACS Catal. 2019, 9, 1464−1471

(17) Perskie, L. L.; Street, T. O.; Rose, G. D. Structures, Basins, and Energies: A Deconstruction of the Protein Coil Library. *Protein Sci.* **2008**, *17*, 1151−1161.
(18) Némethy, G.; Printz, M. P. The γ Turn, a Possible Folded Conformation of the Polypeptide Chain. Comparison with the β Turn. *Macromolecules* **1972**, *5*, 755−758.
(19) Classic γ-turns reverse the direction of the main chain, whereas inverse γ-turns (which are more prevalent) induce a kink in the main chain: Milner-White, E.; Ross, B. M.; Ismail, R.; Belhadj-Mostefa, K.; Poet, R. One Type of Gamma-Turn, Rather Than the Other, Gives Rise to Chain-Reversal in Proteins. *J. Mol. Biol.* **1988**, *204*, 777−782.
(20) Pettit, S. C.; Simsic, J.; Loeb, D. D.; Everitt, L.; Hutchison, C. A., 3rd; Swanstrom, R. Analysis of Retroviral Protease Cleavage Sites Reveals Two Types of Cleavage Sites and the Structural Requirements of the P1 Amino Acid. *J. Biol. Chem.* **1991**, *266*, 14539−14547.
(21) de Oliveira, T.; Engelbrecht, S.; Janse van Rensburg, E.; Gordon, M.; Bishop, K.; zur Megede, J.; Barnett, S. W.; Cassol, S. Variability at Human Immunodeficiency Virus Type 1 Subtype C Protease Cleavage Sites: An Indication of Viral Fitness? *J. Virol.* **2003**, *77*, 9422−9430.
(22) Newlander, K. A.; Callahan, J. F.; Moore, M. L.; Tomaszek, T. A.; Huffman, W. F. A Novel Constrained Reduced-Amide Inhibitor of HIV-1 Protease Derived from the Sequential Incorporation of γ-Turn Mimetics into a Model Substrate. *J. Med. Chem.* **1993**, *36*, 2321−2331.
(23) (a) Moore, M. L.; Dreyer, G. B. Substrate-Based Inhibitors of HIV-1 Protease. *Perspect. Drug Discovery Des.* **1993**, *1*, 85−108. (b) Hoog, S. S.; Zhao, B.; Winborne, E.; Fisher, S.; Green, D. W.; DesJarlais, R. L.; Newlander, K. A.; Callahan, J. F.; Abdel-Meguid, S. S.; Moore, M. L.; Huffman, W. F. A Check on Rational Drug Design: Crystal Structure of a Complex of Human Immunodeficiency Virus Type 1 Protease with a Novel γ-Turn Mimetic Inhibitor. *J. Med. Chem.* **1995**, *38*, 3246−3252.
(24) Wilhelm, P.; Lewandowski, B.; Trapp, N.; Wennemers, H. A Crystal structure of an Oligoproline PPII-Helix, at Last. *J. Am. Chem. Soc.* **2014**, *136*, 15829−15832.
(25) (a) Horng, J.-C.; Raines, R. T. Stereoelectronic Effects on Polyproline Conformation. *Protein Sci.* **2006**, *15*, 74−83. (b) Adzhubei, A. A.; Sternberg, M. J.; Makarov, A. A. Polyproline-II Helix in Proteins: Structure and Function. *J. Mol. Biol.* **2013**, *425*, 2100−2132.
(26) (a) Singh, S. K.; Das, A. The $n\rightarrow\pi^*$ Interaction: A Rapidly Emerging Non-Covalent Interaction. *Phys. Chem. Chem. Phys.* **2015**, *17*, 9596−9612. (b) Newberry, R. W.; Raines, R. T. The $n\rightarrow\pi^*$ Interaction. *Acc. Chem. Res.* **2017**, *50*, 1838−1846.
(27) Bartlett, G. J.; Choudhary, A.; Raines, R. T.; Woolfson, D. N. $n\rightarrow\pi^*$ Interactions in Proteins. *Nat. Chem. Biol.* **2010**, *6*, 615−620.
(28) Shi, Z.; Chen, K.; Liu, Z.; Kallenbach, N. R. Conformation of the Backbone in Unfolded Proteins. *Chem. Rev.* **2006**, *106*, 1877−1897.
(29) Cubellis, M. V.; Caillez, F.; Blundell, T. L.; Lovell, S. C. Properties of Polyproline II, a Secondary Structure Element Implicated in Protein−Protein Interactions. *Proteins: Struct., Funct., Genet.* **2005**, *58*, 880−892.
(30) Brown, A. M.; Zondlo, N. J. A Propensity Scale for Type II Polyproline Helices (PPII): Aromatic Amino Acids in Proline-Rich Sequences Strongly Disfavor PPII Due to Proline−Aromatic Interactions. *Biochemistry* **2012**, *51*, 5041−5051.
(31) Kovalevsky, A. Y.; Chumanevich, A. A.; Liu, F.; Louis, J. M.; Weber, I. T. Caught in the Act: The 1.5 Å Resolution Crystal Structures of the HIV-1 Protease and the I54V Mutant Reveal a Tetrahedral Reaction Intermediate. *Biochemistry* **2007**, *46*, 14854−14864.
(32) Windsor, I. W.; Raines, R. T. A Substrate Selected by Phage Display Exhibits Enhanced Side-Chain Hydrogen Bonding to HIV-1 Protease. *Acta Crystallogr.* **2018**, *D74*, 690−694.
(33) Coates, L.; Tuan, H. F.; Tomanicek, S.; Kovalevsky, A.; Mustyakimov, M.; Erskine, P.; Cooper, J. The Catalytic Mechanism of an Aspartic Proteinase Explored with Neutron and X-ray Diffraction. *J. Am. Chem. Soc.* **2008**, *130*, 7235−7237.
(34) (a) Weinhold, F.; Landis, C. R. *Discovering Chemistry with Natural Bond Orbitals*; John Wiley & Sons: Hoboken, NJ, 2012. (b) Weinhold, F. Natural Bond Orbital Analysis: A Critical Overview of Relationships to Alternative Bonding Perspectives. *J. Comput. Chem.* **2012**, *33*, 2363−2379.
(35) Choudhary, A.; Fry, C. G.; Kamer, K. J.; Raines, R. T. An $n\rightarrow\pi^*$ Interaction Reduces the Electrophilicity of the Acceptor Carbonyl Group. *Chem. Commun.* **2013**, *49*, 8166−8168.
(36) (a) Henderson, R. Structure of Crystalline α-Chymotrypsin. IV. The Structure of Indoleacryloyl-α-Chymotrypsin and Its Relevance to the Hydrolytic Mechanism of the Enzyme. *J. Mol. Biol.* **1970**, *54*, 341−354. (b) Henderson, R.; Wright, C. S.; Hess, G. P.; Blow, D. M. α-Chymotrypsin: What Can We Learn About Catalysis from X-ray Diffraction? *Cold Spring Harbor Symp. Quant. Biol.* **1972**, *36*, 63−69. (c) Robertus, J. D.; Kraut, J.; Alden, R. A.; Birktoft, J. Subtilisin; a Stereochemical Mechanism Involving Transition-State Stabilization. *Biochemistry* **1972**, *11*, 4293−4303. (d) Kraut, J. Serine Proteases: Structure and Mechanism of Catalysis. *Annu. Rev. Biochem.* **1977**, *46*, 331−358. (e) Bryan, P.; Pantoliano, M. W.; Quill, S. G.; Hsiao, H.-Y.; Poulos, T. Site-Directed Mutagenesis and the Role of the Oxyanion Hole in Subtilisin. *Proc. Natl. Acad. Sci. U. S. A.* **1986**, *83*, 3743−3745.
(37) Simon, L.; Goodman, J. M. Enzyme Catalysis by Hydrogen Bonds: The Balance Between Transition State Binding and Substrate Binding in Oxyanion Holes. *J. Org. Chem.* **2010**, *75*, 1831−1840.
(38) (a) Pauling, L. Molecular Architecture and Biological Reactions. *Chem. Eng. News* **1946**, *24*, 1375−1377. (b) Pauling, L. Chemical Achievement and Hope for the Future. *Am. Sci.* **1948**, *36*, 51−58. (c) Pauling, L. Nature of Forces Between Large Molecules of Biological Interest. *Nature* **1948**, *161*, 707−709. (d) Jencks, W. P. Strain and Conformation Change in Enzymatic Catalysis. In *Current Aspects of Biochemical Energetics*; Kaplan, N. O., Kennedy, E. P., Eds. Academic Press: New York, NY, 1966; pp 273−298. (e) Lienhard, G. E. Enzymatic Catalysis and Transition-State Theory. *Science* **1973**, *180*, 149−154. (f) Albery, W. J.; Knowles, J. R. Evolution of Enzyme Function and the Development of Catalytic Efficiency. *Biochemistry* **1976**, *15*, 5631−5640.
(39) (a) Pauling, L. In *Nature of the Chemical Bond*; Cornell University Press: Ithaca, NY, 1939; pp 192−193. (b) Pearl, L. H. The Catalytic Mechanism of Aspartic Proteases. *FEBS Lett.* **1987**, *214*, 8−12. (c) Kirby, A. J.; Komarov, I. V.; Wothers, P. D.; Feeder, N. The Most Twisted Amide: Structure and Reactions. *Angew. Chem., Int. Ed.* **1998**, *37*, 785−786. (d) Mujika, J. I.; Mercero, J. A.; Lopez, Z. Water-Promoted Hydrolysis of a Highly Twisted Amide: Rate Acceleration Caused by the Twist of the Amide Bond. *J. Am. Chem. Soc.* **2005**, *127*, 4445−4453. (e) Aube, J. A. New Twist on Amide Solvolysis. *Angew. Chem., Int. Ed.* **2012**, *51*, 3063−3065.
(40) Tözsér, J.; Bláha, I.; Copeland, T. D.; Wondrak, E. M.; Oroszlan, S. Comparison of the HIV-1 and HIV-2 Proteinases Using Oligopeptide Substrates Representing Cleavage Sites in Gag and Gag-Pol Polyproteins. *FEBS Lett.* **1991**, *281*, 77−80.
(41) Potempa, M.; Lee, S.-K.; KurtYilmaz, N.; Nalivaika, E. A.; Rogers, A.; Spielvogel, E.; Carter, C. W.; Schiffer, C. A.; Swanstrom, R. HIV-1 Protease uses Bi-Specific S2/S2′ Subsites to Optimize Cleavage of Two Classes of Target Sites. *J. Mol. Biol.* **2018**, *430*, 5182−5195.
(42) (a) Carnevale, V.; Raugei, S.; Piana, S.; Carloni, P. On the Nature of the Reaction Intermediate in the HIV-1 Protease: A Quantum Chemical Study. *Comput. Phys. Commun.* **2008**, *179*, 120−123. (b) Garrec, J.; Sautet, P.; Fleurat-Lessard, P. Understanding the HIV-1 Protease Reactivity with DFT: What Do We Gain from Recent Functionals? *J. Phys. Chem. B* **2011**, *B115*, 8545−8558. (c) Ribeiro, A. J. M.; Santos-Martins, D.; Russo, N.; Ramos, M. J.; Fernandes, P. A. Enzymatic Flexibility and Reaction Rate: A QM/MM study of HIV-1 Protease. *ACS Catal.* **2015**, *5*, 5617−5626. (d) Krzemińska, A.; Moliner, V.; Świderek, K. Dynamic and Electrostatic Effects on the Reaction Catalyzed by HIV-1 Protease. *J. Am. Chem. Soc.* **2016**, *138*, 16283−16298.
(43) (a) Kipp, D. R.; Hirschi, J. S.; Wakata, A.; Goldstein, H.; Schramm, V. L. Transition States of Native and Drug-Resistant HIV-1

DOI: 10.1021/acscatal.8b04142
ACS Catal. 2019, 9, 1464−1471

Protease are the Same. *Proc. Natl. Acad. Sci. U. S. A.* **2012**, *109*, 6543−6548. (b) Bras, N. F.; Ramos, M. J.; Fernandes, P. A. The Catalytic Mechanism of Mouse Renin Studied with QM/MM Calculations. *Phys. Chem. Chem. Phys.* **2012**, *14*, 12605−12613. (c) Calixto, A. R.; Brás, N. F.; Fernandes, P. A.; Ramos, M. J. Reaction Mechanism of Human Renin Studied by Quantum Mechanics/Molecular Mechanics (QM/MM) Calculations. *ACS Catal.* **2014**, *4*, 3869−3876.

(44) Calixto, A. R.; Ramos, M. J.; Fernandes, P. A. Influence of Frozen Residues on the Exploration of the PES of Enzyme Reaction Mechanisms. *J. Chem. Theory Comput.* **2017**, *13*, 5486−5495.

(45) Recently, we described a role for S···C═O $n\rightarrow\pi^*$ interactions in catalysis by thioredoxin and other enzymes that employ a CXXC motif (Kilgore, H. R.; Raines, R. T. $n\rightarrow\pi^*$ Interactions Modulate the Properties of Cysteine Residues and Disulfide Bonds in Proteins. *J. Am. Chem. Soc.* **2018**, DOI: 10.1021/jacs.8b09701).

(46) Tomasi, J.; Mennucci, B.; Cammi, R. Quantum Mechanical Continuum Solvation Models. *Chem. Rev.* **2005**, *105*, 2999−3093.

(47) Frisch, M. J.; Trucks, G. W.; Schlegel, H. B.; Scuseria, G. E.; Robb, M. A.; Cheeseman, J. R.; Scalmani, G.; Barone, V.; Petersson, G. A.; Nakatsuji, H.; Li, X.; Caricato, M.; Marenich, A. V.; Bloino, J.; Janesko, B. G.; Gomperts, R.; Mennucci, B.; Hratchian, H. P.; Ortiz, J. V.; Izmaylov, A. F.; Sonnenberg, J. L.; Williams-Young, D.; Ding, F.; Lipparini, F.; Egidi, F.; Goings, J.; Peng, B.; Petrone, A.; Henderson, T.; Ranasinghe, D.; Zakrzewski, V. G.; Gao, J.; Rega, N.; Zheng, G.; Liang, W.; Hada, M.; Ehara, M.; Toyota, K.; Fukuda, R.; Hasegawa, J.; Ishida, M.; Nakajima, T.; Honda, Y.; Kitao, O.; Nakai, H.; Vreven, T.; Throssell, K.; Montgomery, J. A., Jr.; Peralta, J. E.; Ogliaro, F.; Bearpark, M. J.; Heyd, J. J.; Brothers, E. N.; Kudin, K. N.; Staroverov, V. N.; Keith, T. A.; Kobayashi, R.; Normand, J.; Raghavachari, K.; Rendell, A. P.; Burant, J. C.; Iyengar, S. S.; Tomasi, J.; Cossi, M.; Millam, J. M.; Klene, M.; Adamo, C.; Cammi, R.; Ochterski, J. W.; Martin, R. L.; Morokuma, K.; Farkas, O.; Foresman, J. B.; Fox, D. J. *Gaussian 16*, Revision A.03; Gaussian, Inc.: Wallingford, CT, 2016.

(48) Glendening, E. D.; Badenhoop, J. K.; Reed, A. E.; Carpenter, J. E.; Bohmann, J. A.; Morales, C. M.; Landis, C. R.; Weinhold, F. *NBO 6.0*; Theoretical Chemistry Institute, University of Wisconsin−Madison: Madison, WI, 2013.

(49) Wendt, M.; Weinhold, F. *NBOView 1.1*; Theoretical Chemistry Institute, University of Wisconsin−Madison: Madison, WI, 2001.

DOI: 10.1021/acscatal.8b04142
ACS Catal. 2019, 9, 1464−1471